Rare Metal Materials and Engineering
Volume 49, Issue 11, November 2020
Available online at www.rmme.ac.cn

Science Press

Cite this article as: Rare Metal Materials and Engineering, 2020, 49(11): 3741-3747.

ARTICLE

Preparation and Mechanical Properties of ZL205A Alloy-Infiltrated SiC Foam Ceramic Composites

Qi Yushi[1], Wang Yanbo[2], Du Lanjun[3], Fei Yanhan[1], Du Zhiming[1]

[1] School of Materials Science and Engineering, Harbin Institute of Technology, Harbin 150001, China; [2] Shanghai Spaceflight Precision Machinery Institute, Shanghai 201600, China; [3] Beijing Aerospace Propulsion Institute, Beijing 100076, China

Abstract: ZL205A alloy-infiltrated SiC foam ceramic composites were prepared by extrusion infiltration process. The effect of different porosity of SiC foam ceramic on the properties of the composites was investigated. The results show that the prepared SiC foam ceramics are tightly combined with the ZL205A matrix material, and there are few cracks and other defects can be observed. The SiC foam ceramic as the reinforcing phase refines the grains of the ZL205A matrix phase. The pore structure and the grain size are finer and smaller with the decrease of reinforcing phase porosity. The mechanical properties of the ZL205A alloy-infiltrated SiC foam ceramic composites were investigated. The hardness (HV) and flexural strength of the composites are 1276 MPa and 415 MPa, respectively. The wear resistance of the composites was also investigated. The results demonstrate that the addition of ceramic reinforcing phase can effectively transform the severe adhesive wear and spalling wear of the matrix phase into lighter abrasive wear, which greatly improves the friction and wear properties of the composites.

Key words: SiC foam ceramic; ZL205A alloy; extrusion infiltration process

Al alloy has attracted more attention due to its perfect ductility, environmental friendliness and ease to recycling. However, the low specific stiffness, hardness and poor wear resistance limit its applications in the engineering field [1, 2]. Ceramic materials have high specific strength, outstanding hardness and wear resistance. Thus, researchers put forward the metal matrix composite (MMC), and the ceramic-metal composites have considerable application prospects, which combines the advantages of metal and ceramic material [3-6]. Ceramic reinforcing phase usually consists of ceramic particle, ceramic fiber and ceramic foam with three-dimension structure. Ceramic particle and ceramic fiber may have uneven distribution in metal matrix, which will be detrimental to the properties of composite. Fortunately, ceramic foam as the reinforcing phase could effectively solve this problem because of its special network topology structure [7-10].

Extrusion infiltration process is commonly used to prepare ceramic form-reinforced metal matrix composite[11]. During the process, pressure is applied to the molten metal liquid, which is then infiltrated into the ceramic foam. The process schematic is shown in Fig.1[12]. The advantages of this technology are that the molten metal liquid can be infiltrated into the ceramic foam with a high speed, and this process eliminates the effect of capillary action. In addition, compared with other infiltration technology, extrusion infiltration process needs lower infiltration temperature, which can inhibit adverse interface production and improve composite property[13-16].

The paper prepared ZL205A alloy-infiltrated SiC foam ceramic composite by extrusion infiltration process, and investigated the effect of different porosities of SiC foam ceramic on the properties of composite.

1 Experiment

ZL205A alloy (Northeast Light Alloy Co., Ltd, China) was used as experimental blank with dimensions of 50 mm×

Received date: November 25, 2019
Corresponding author: Du Zhiming, Ph. D., Professor, School of Materials Science and Engineering, Harbin Institute of Technology, Harbin 150001, P. R. China, E-mail: duzm@263.net

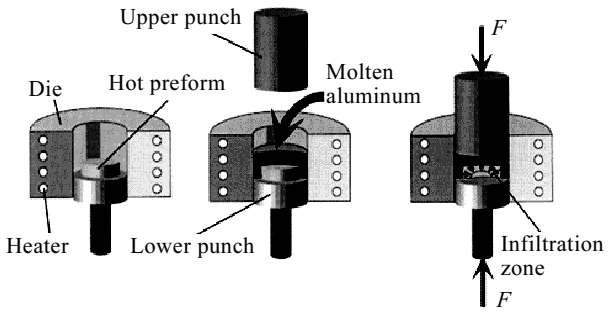

Fig.1 Schematic of extrusion infiltration process[12]

70 mm×150 mm. The composition of the blank measured by X-ray fluorescence spectrometer (AXIOS-PW4400) is shown in Table 1. SiC foam ceramics with 85vol%, 80vol% and 75vol% porosity were the reinforcing phase. The photographs of SiC foam ceramics are shown in Fig.2. SiC foam ceramics were rinsed with the distilled water under ultrasonic wave to eliminate the effect of the surface impurities, and then were dried at 120 °C in a vacuum oven for 24 h. Before infiltration process, SiC foam ceramics were pre-heated in an electric furnace at 300 °C, and ZL205A alloy was melted in a well type furnace at 720 °C. During the infiltration process, the pre-heated SiC foam ceramic was placed in the mold, and subsequently the molten alloy liquid was poured into the mold. It was made sure that the alloy liquid submerged the foam ceramic. Infiltration process was conducted on a 2000 kN hydropress (THP16-200), and the alloy liquid was pushed into the foam ceramic under the pressure of 20 MPa with the duration of 30 s.

The wear resistance, mechanical properties and microstructure of the composites were characterized by the frictional wear test, three-point bending test, optical microscope (OM) and scanning electron microscope (SEM) with energy dispersive spectroscopy (EDS). The composite phase was tested by a D/MAX-RB X-ray diffraction (XRD) system with Cu Kα radiation. The tube voltage and current are 40 kV and 40 mA, respectively. The friction and wear test were performed on a pin-disk friction and wear tester (YTH TB-1000) at room temperature in air. The grinding disc made of GCr15 bearing steel rotated at a linear velocity of 1.6 m/s and a friction distance of 2000 m. In the friction and wear test, the samples (5 mm×5 mm×15 mm) were firmly fixed on the fixture of the testing machine, and a normal load of 30 N was applied to the sample surface. Flexural strength was measured by an electronic universal material testing machine (AG-Xplus 250 kN).

2 Results and Discussion

2.1 Microstructure of the prepared composites

Microstructure of the prepared composites 85C, 80C and 75C, which denote the composites with 85vol%, 80vol% and 75vol% porosity ceramic reinforcing phases, respectively, are shown in Fig.3. In Fig.3a~3c, the ZL205A grain becomes finer with the decrease of ceramic reinforcing phase porosity. This can be ascribed to the larger temperature gradient and small liquid convection. In composite 75C, the larger interfaces between the ceramic and alloy liquid also make the release of the crystallize latent heat more easy. Furthermore, the ceramic bones are intensive and slender in 75C, which are facilitated to break up the coarse dendrite and refine the grains. In composites with small porosity (75C), the size of the grains near the ribs is larger than that of the grains far away from the ribs, which is converse to that of the composites with high porosity. In composite 85C, the size of the grains near the ribs is smaller than that of the grains far away from the ribs. This can be attributed to the larger temperature gradient, which derives from the intense instantaneous thermal conductivity of the sturdy ceramic bones. In Fig.3d~3f, the micro holes and cracks can be obviously observed, which is beneficial to improve the composite mechanical properties.

Table 1 Chemical composition of ZL205A (wt%)

Cu	Ti	Zr	V	Mn	Cd	Al
5.16	0.19	0.17	0.23	0.40	0.24	93.61

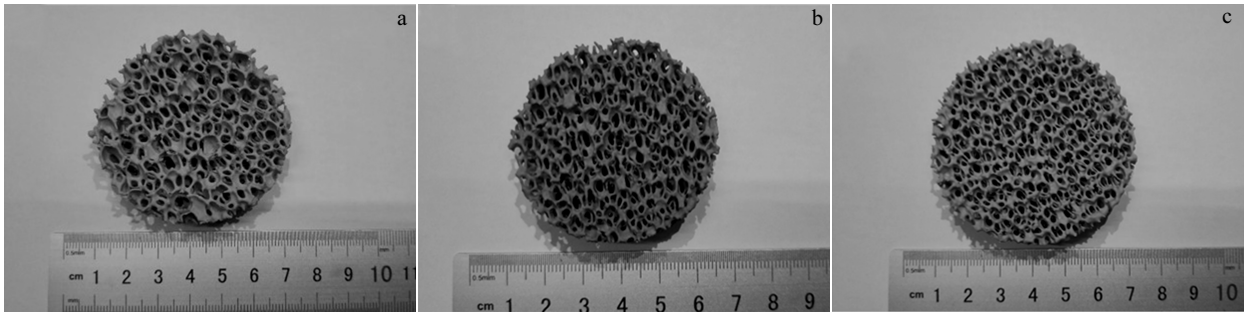

Fig.2 Photographs of SiC foam ceramics with different porosities: (a) 85 vol%, (b) 80 vol%, and (c) 75 vol%

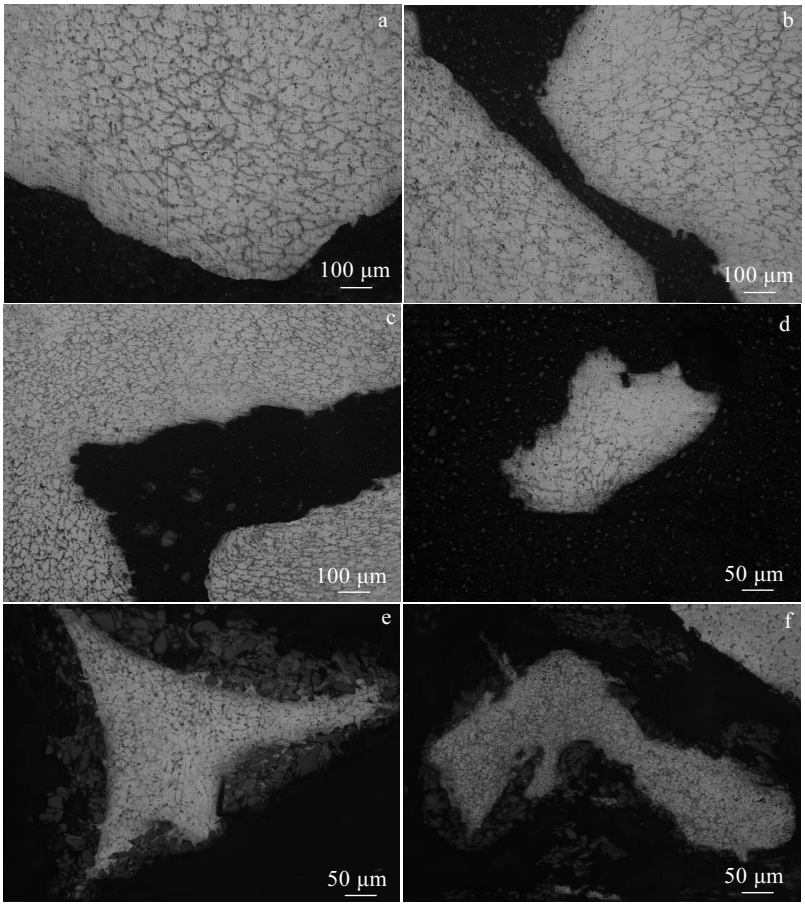

Fig.3 Microstructures of the prepared composites: (a) 85C, (b) 80C, (c) 75C, and (d~f) different positions in 85C

SEM image and EDS analysis of points 1~4 in the 85C composites are shown in Fig.4. Fig.4b demonstrates the EDS analysis of point 1 (SiC ceramic reinforcing phase), and Al, O, Si, C and little Cu is detected. Al and a large proportion of O come from the Al_2O_3, which is the sintering additive for the SiC ceramics. There are also some O elements deriving from SiO_2, which is the oxidation product of SiC. The SiO_2 can react with Al_2O_3 to form mullite phase, which as a reinforcement phase can improve the composite mechanical properties. At point 2, some strip-shaped product can be observed. Cu element is detected in this area, as shown in Fig.4c. This can be ascribed to the Cu beneficiation on the grain boundary, and the AlCu precipitation on the grain boundary during the solidification. In addition, the existence of O element indicates that the oxidation occurs in this area. Fig.4d shows the EDS analysis of point 3, which is located at the interface between ceramic and alloy phase. The peaks of Al and Si are intense, and the content of the Al and Si are 66.61% and 16.57%, respectively. In Fig.4e, only Al and O can be detected, which demonstrates that the alloy matrix is oxidized slightly during the process.

Fig.5 presents the SEM image and EDS analysis of the area away from the ceramic reinforcing phase. There are also a large number of strip-shaped products. Fig.5c and Fig.5d indicate that the strip-shaped products are AlCu which are precipitated on the grain boundary. The XRD patterns of the as-prepared composites are shown in Fig.6. The detection of AlCu, $CuSiO_3$, $SiAl_4$ phases (PDF standard cards are 88-1713, 82-1403 and 79-0988, respectively) indicates the element diffusion between ZL205A alloy and SiC reinforcing phase.

2.2 Mechanical properties of the prepared composites

Mechanical properties of the prepared composites and ZL205A alloy matrix are shown in Table 2. In hardness test, the test positions are chosen in alloy matrix, which are away from the ceramic phase. The 75C composite displays the largest hardness (HV) (1276 MPa), and the smallest hardness of the 85C composites is 705 MPa, which is also larger than that of the ZL205A alloy matrix (528 MPa). This can be ascribed to that the addition of ceramics phase refines the alloy grain, which is consistent with the composite microstructure in Fig.3. The flexural strength of the prepared composite increases with the increase of porosity. The flexural strength of the 75C and 85C are 367.5 MPa and

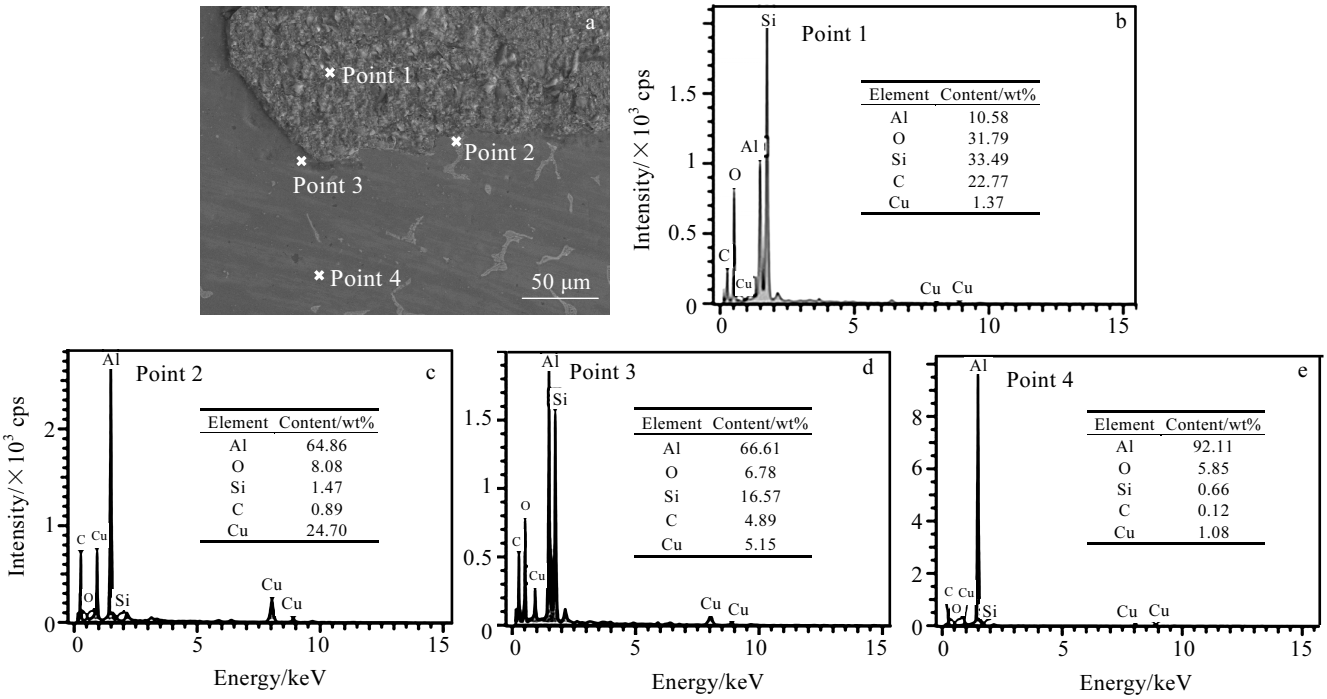

Fig.4 SEM image (a) of 85C composite and EDS analysis (b~e) of the points 1~4 in Fig.4a

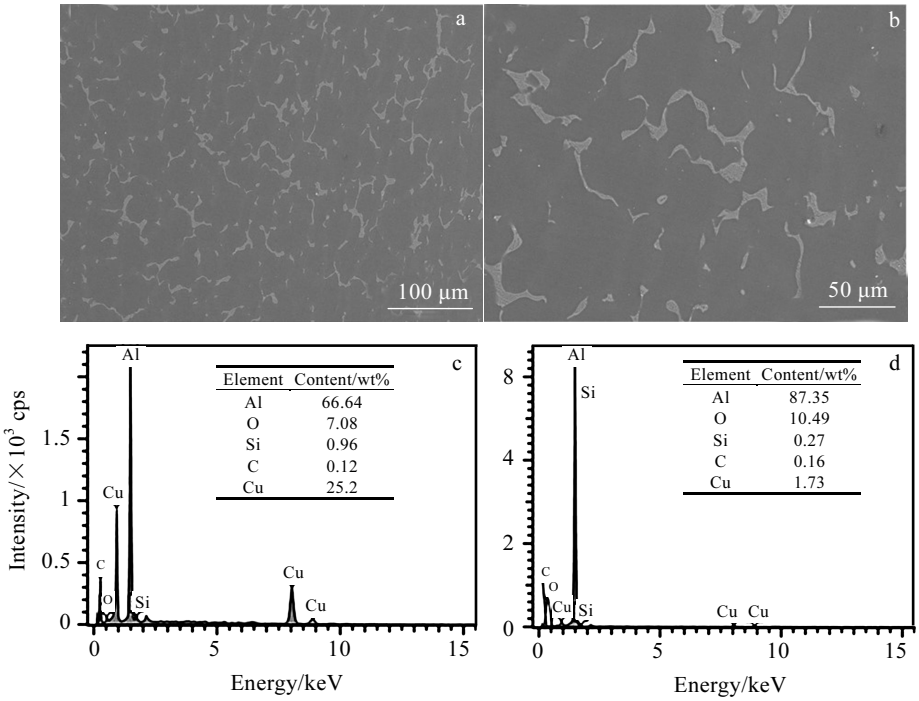

Fig.5 SEM images (a, b) and EDS analysis (c, d) of strip-shaped products for 85C composite

Table 2 Mechanical properties of the prepared composites and ZL205A alloy matrix

Sample	Hardness, HV/MPa	Flexural strength/MPa	Relative density/%
75C	1276	367.5	96.15
80C	977	379.8	94.24
85C	705	415.7	96.37
ZL205A	528	-	-

415.7 MPa, respectively. There are more interfaces between ceramic bones and alloy matrix in 75C, so more defects will be generated during the text. Furthermore, the ceramic bones in 75C are thinner than those in 85C, which are detrimental to the mechanical properties.

2.3 Wear resistance of the prepared composites

Fig.7 presents the wear rate and coefficient of friction of the prepared composite and ZL205A alloy matrix. The co-

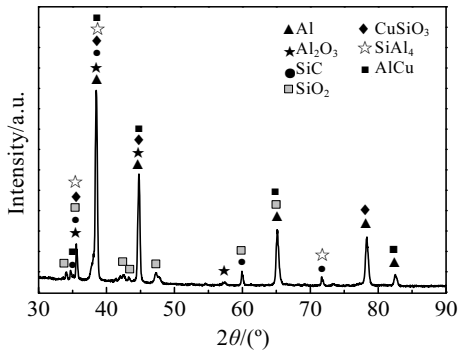

Fig.6 XRD pattern of 85C composite

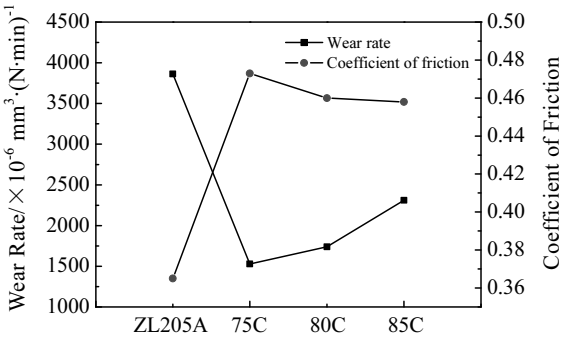

Fig.7 Wear rate and coefficient of friction of the prepared composites and ZL205A alloy matrix

efficient of friction of the ZL205A alloy matrix is 0.365, which is lower than that of the composite. The largest coefficient of friction of the composite is 0.473 (75C), and the coefficient of friction decreases with the increase of the ceramic porosity. This can be ascribed to that the small porosity ceramic reinforcing phase (75C) has much ceramic bones and dense microstructure, which will increase the contact surface between the ceramic and the grinding disc. Influence factor of contact surface on ceramic coefficient of friction is set to be λ, and the composite coefficient of friction μ_0 can be calculated through the following formula:

$$\mu_0=\lambda\mu_1+(1-\lambda)\mu_2 \quad (1)$$

Where $1-\lambda$ is the influence factor of contact surface on ZL205A matrix coefficient of friction, μ_1 and μ_2 are the coefficient of friction of ceramic and ZL205A matrix, respectively. The lowest wear rate of the composite is 1527.51×10^{-6} $mm^3/(N\cdot min)$, which is much lower than the half of the wear rate of the ZL205A matrix (3862.48×10^{-6} $mm^3/(N\cdot min)$).

2.4 Discussion of the wear resistance of the prepared composites

Fig.8 demonstrates the SEM images of the ZL205A alloy matrix after wear resistance test. In Fig.8a, there are some obvious scratches and grooves, and some abrasive dust is also can be found in the scratches along the wear side. These are the typical characteristics belonging to adhesive wear mechanism. Some stripping pits can be observed besides scratches and grooves, as shown in Fig.8b, which indicates the effect of spalling wear mechanism. During the wear test, defects such as cracks form because of the load pressure along the normal and the friction force along the tangential. The fragment will be stripped out from the matrix when these defects extend to the contact surface. Micro cracks on subsurface after exfoliation and obvious scratches on surface could be detected, as shown in Fig.8c. Fig.8d shows that a great number of abrasive dust form in the

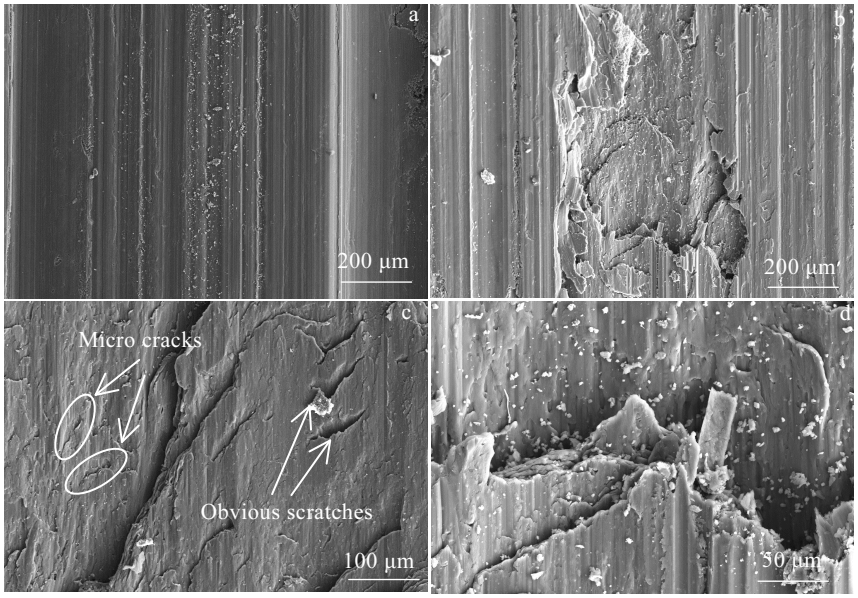

Fig.8 SEM images of the ZL205A alloy matrix after wear resistance test: (a, b) scratches, grooves and dusts; (c, d) micro cracks and abrasive dusts

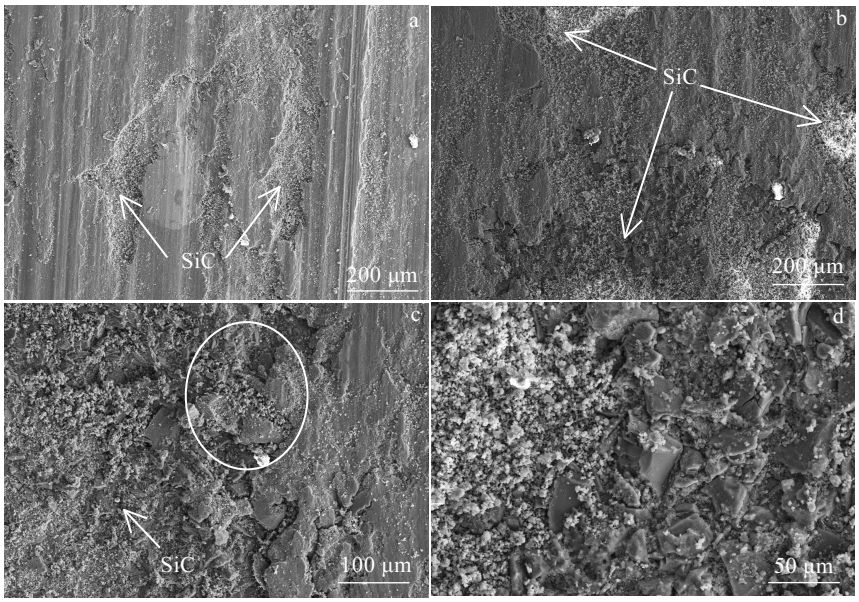

Fig.9 SEM images of the prepared composites after wear resistance test: (a, b) ceramic reinforcing phase and (c, d) abrasive dusts

boundary between surface and subsurface. This can be ascribed to the matrix softening and surface spalling because of high temperature during wear resistance test.

Fig.9 presents the SEM images of the prepared composite after wear resistance test. At the initial stage of wear resistance test, the composite exhibits serious abrasion. This is because the ZL205A alloy matrix is the main wear-resistant material at this stage. With the test proceeding, SiC ceramic reinforcing phase is observed and the wear scratches around the ceramic phase become weaker, as shown in Fig.9a. The SiC ceramic reinforcing phase which possesses high hardness sustains the main load pressure along the normal and the friction force along the tangential at this stage. No obvious scratch and crack could be observed in Fig.9b, which indicates that the adhesive wear mechanism is weakened. In Fig.9c, some abrasive dust accumulates in convex position marked in the white circle. These abrasive dusts will form incompressible points and strip off the convex position, which are detrimental to the wear resistance property. However, the existence of the ceramic reinforcing phase would distribute the abrasive dust to eliminate the effect of abrasive dust accumulation[17, 18]. Above all, not only the addition of SiC ceramic reinforcing phase can improve the composite wear resistance, but the coaction of ceramic reinforcing phase and alloy matrix are facilitated to the composite wear resistance as well.

3 Conclusions

1) ZL205A alloy-infiltrated SiC foam ceramic composites are successfully prepared by extrusion infiltration process. The elements diffusion occurs at the interface between SiC foam ceramics and ZL205A matrix material, and there are few cracks and other defects can be observed.

2) The largest hardness (HV) and flexural strength of the composites are 1276 MPa and 415.7 MPa, respectively. The SiC foam ceramic as the reinforcing phase refines the grains of the ZL205A matrix phase.

3) The 75C composite possesses the best wear resistance. The largest coefficient of friction and the lowest wear rate are 0.473 and 1527.51×10^{-6} $mm^3/(N\cdot min)$, respectively.

4) The ceramic reinforcing phase can effectively transform the severe adhesive wear and spalling wear of the alloy matrix phase into lighter abrasive wear.

References

1 Han G W, Feng D, Yin M *et al. Materials Science & Engineering A*[J], 1997, 225(1-2): 204
2 Wu C M L, Han G W. *Materials Characterization*[J], 2007, 58(5): 416
3 Liu Shaobo, Li Aiqun. *Composite Structures*[J], 2018, 203: 18
4 Wang Q, Zhang H, Cai H *et al*. *Computational Materials Science*[J], 2017, 129: 123
5 Wang Hao, Chen Ziwei, Liu Lili *et al*. *Ceramics International*[J], 2018, 44(9): 10 078
6 Ge Xuexiang, Zhou Mingkai, Wang Huaide. *Ceramics International*[J], 2019, 45(9): 12 528
7 Hou Lijun, Liu Taoyong, Lu Anxian. *Transactions of Nonferrous Metals Society of China*[J], 2017, 27(3): 591
8 Tripathy S, Saini D S, Bhattacharya D. *Journal of Asian Ceramic Societies*[J], 2016, 4(2): 149
9 Martin C, Zdenek C, Adam S *et al. Journal of the European Ceramic Society*[J], 2015, 35(13): 3427
10 Li Y, Cheng X D, Gong L L *et al. Journal of the European Ceramic Society*[J], 2015, 35(1): 267

11 Liu Q, Ye F, Gao Y *et al*. *Journal of Alloys and Compounds*[J], 2014, 585: 146
12 Wagner F, Garcia D E, Krupp A *et al. Journal of the European Ceramic Society*[J], 1999, 19(13-14): 2449
13 Gregolin E N, Goldenstein H, Santos R G. *Journal of Materials Processing Technology*[J], 2014, 157-158: 688
14 Lu Y, Yang J, Lu W *et al*. *Materials Science & Engineering A*[J], 2010, 527(23): 6289
15 Zhu Jianbin, Yan Hong. *Ceramics International*[J], 2017, 43(15): 12996
16 Zhu J, Wang F, Wang Y *et al. Ceramics International*[J], 2017, 43(8): 6563
17 Lu Zhi. *Thesis for Doctorate*[D]. Changsha: Central South University, 2013 (in Chinese)
18 Chen Ke. *Thesis for Master*[D]. Harbin: Harbin Institute of Technology, 2012 (in Chinese)

SiC 泡沫陶瓷增强 ZL205A 铝合金复合材料的制备与性能

綦育仕[1]，汪彦博[2]，杜兰君[3]，费岩晗[1]，杜之明[1]
(1. 哈尔滨工业大学 材料科学与工程学院，黑龙江 哈尔滨 150001)
(2. 上海航天精密机械研究所，上海 201600)
(3. 北京航天动力研究所，北京 100076)

摘　要：通过挤压浸渗工艺成功制备了 SiC 泡沫陶瓷增强 ZL205A 铝合金复合材料，并研究了不同孔隙率的泡沫陶瓷增强相对复合材料性能的影响。通过微观结构分析，制备的复合材料两相间结合紧密，没有裂纹及其他缺陷产生。多孔陶瓷作为增强相可以有效地细化 ZL205A 合金的晶粒，多孔陶瓷孔隙率降低，孔结构越小，合金晶粒越细小。对制备的复合材料进行力学性能测试，复合材料的硬度（HV）和抗弯强度最高能够达到 1276 MPa 和 415 MPa。对制备的复合材料进行摩擦磨损测试。结果表明，连续陶瓷相的存在将铝基体严重的粘着磨损和剥落磨损转变为较轻的磨粒磨损，极大提升了复合材料的摩擦磨损性能，为其用于耐磨领域提供了理论依据。

关键词：SiC 泡沫陶瓷；ZL205A 铝合金；挤压浸渗工艺

作者简介：綦育仕，男，1991 年生，博士，哈尔滨工业大学材料科学与工程学院，黑龙江 哈尔滨 150001，E-mail: qys_gd@sina.cn